SPATIAL VARIATION OF BENO-A-PYRENE, NICKEL AND LEAD CONFINED IN PM10 AS WELL MODELLING AND HEALTH RISK ASSESSMENT

Devolakshi Handique* and Krishna G. Bhattacharyya
Department of Chemistry, Gauhati University, Guwahati, Assam 781014, India
*For correspondence. (handiquedevolakshi@gmail.com)

Abstract: Exposure to fine particulate matter from ambient air is a leading environmental contributor to disease burden across the world. Polycyclic aromatic hydrocarbons (PAHs) are the common environmental pollutants. PAHs are persistent organic pollutants and strive carcinogenic and mutagenic effects. Aerosol samples in the particulate phase were collected simultaneously for the first time in Numaligarh at an industrial and a traffic dominated site for two year to investigate the gas–particle partitioning of polycyclic aromatic hydrocarbon (PAH) and heavy metal. The samples were collected using a high volume sampler on PTFE filter papers. Benzo-a-pyrene was analyzed using gas chromatograph-mass spectrometry. The ground level concentration (GLC) of pollutants from stationary sources is computed using dispersion model AERMOD, which are mathematical relations between the source strength and concentration and involves parameters related transport and diffusion. Increases in GLC (Ground Level Concentration) are very minimal. Maximum Predicted Summer Season 24 hour Average increase in GLC is 2.05 μgm^{-3} and that of winter is 1.58 μgm^{-3}. Although PAH represented a high proportion of risk as carcinogenic whose Cancer Risk (CR) values were calculated (0.03 CR value), and they were very less than the permissible limit (CR > 0.25). However, the risk of exposure to mixtures is difficult to estimate, and risk assessment by whole mixture potency evaluations has been done in this study.

Keywords: PM10; benzo-a-pyrene; lead; nickel; AERMOD; cancer risk

1. Introduction:

Industrial sites are generally important for economic development. The environmental quality in these areas significantly influences economic growth and social progress at regional and larger scales [1]. The group of chemical compounds called as polycyclic aromatic hydrocarbons (PAHs) represents an important class of compounds that contributes to the overall hydrocarbon load in the environment [2]. Seismic survey, oil production as well as refining extracts hydrocarbons that results to considerable impact on the environment [3]. Benzo-a-pyrene as a chemical is of great concern because of its widespread distribution and several impacts on the environment and human health. They may contribute to the formation of ground-level ozone and photochemical smog, which can cause damage to plants and materials. Benzo (a) pyrene (BaP) is one of the most potent carcinogens. This can be measured in both vapour phase and particulate phase. In the vapour phase the concentration of BaP is significantly less than the particulate phase. Therefore care to be taken for the measurement of BaP in the particulate phase [4].

Airborne particles can be defined as ambient airborne particulate matter (PM) which is grouped as coarse, fine and ultrafine particles with aerodynamic diameters within 2.5 to 10 μm (PM10), < 2.5 μm (PM2.5), and < 0.1 μm (PM0.1), respectively. Among other environmental pollutants, airborne particles have been highlighted as a crucial type of pollutant in past several decades. Air pollution causes adverse effects to human bodies through realistic exposures by airborne particles. The PM2.5 (defined as the particulate matter levels of up to 2.5 μm in diameter) is used to reflect the daily air pollution level. Numerous studies have documented the association of PM2.5 air pollution exposure with the morbidity and mortality from respiratory and cardiovascular disease [5]. There were strong evidences that specific diseases including asthma, chronic obstructive pulmonary disease (COPD), pulmonary fibrosis, cancer, type-2 diabetes, neurodegenerative diseases and even obesity could attribute to PM2.5 exposure [6, 7].

Heavy metals contamination is in interest among the scientific community, because of its toxic effects on the entire biosphere Studying of heavy metal pollution found to cause severe illness and sudden death in human

beings for many centuries. It can be in many form such as air, water or soil and can result from automobile exhaust, agriculture, industries and mining activities among others [8]. Anthropogenic activity is one of the most important sources of heavy metal pollution. Vehicular traffic is human induce activity and a major source of contaminants release into the natural environment [9]. The worldwide high vehicular traffic density has led to accelerate emission rates, causing contamination of roadside soils [10]. Cadmium, chromium, nickel, lead and arsenic are mainly released from car exhaust, worn tires and engine parts, brake pads, rust, used antifreeze, road paint and pavement degradation [11, 12]. According to USEPA (1996), half of suspended solids and one sixth of hydrocarbons reaching streams are originated from highways. Tire treads and tire dust contain significant concentration of Zn, brake linings and rubber have high content of Cd, Cu, Fe, Ni, Pb and Zn [13, 14]. High level of heavy metals such as Cd, Co, Cr, Cu, Fe, Pb and Zn have also been reported in many articles, due to the consumption of gasoline, motor oil or grease and antifreeze [15, 16].

In this study, the PM10, benzo-a-pyrene and heavy metal (Pb and Ni) concentrations in Numaligarh were collected for two years. The main objectives of this study were to investigate the spatial and temporal variations of the pollutants in the ambient air at Numaligarh, distinguish between the possible sources of pollution using analysis techniques such as AERMOD, and assess the health risk assessment.

2. Materials and method:

2.1. Study area:

Numaligarh refinery limited situated in Numaligarh is one of medium oil refinery producing 3 million ton crude oil in every year enclosed in north-eastern India and is located in the state of Assam. Numaligarh refinery limited is surrounded by Kajiranga National Park (famous for one horned rhinocerous) and Golaghat town. Many industries like tea and brick manufacturing industries have been built along the refinery. These industries potentially increase the pollutant level in the ambient air. Two sampling sites were selected in Numaligarh with co-ordinates 26º35′2.3″ N, S1 site, 93º46′42.7″E and other one with co-ordinates 26º33′42.1″N, 93º46′35″E, S2 site. Station 1 is located in front of the refinery gate. Station 2 is located at aerial distance of 4km toward south, which serves as a pathway for transportation to Golaghat town at distance of 32 km. This location encompasses different potential sources of anthropogenic activities as it is located near most industrialized area. Each monthly expedition was carried out during the two year i.e. Year 1(Y1) and Year 2(Y2). Ninth times in a month (twice in week) basis samples were collected to determine the concentrations of particulate matter 10, benzo-a-pyrene and heavy metals (Pb and Ni) in the ambient air. All samples were collected in plastic zip lock beg. The samples were then placed in desiccators prior to analysis.

2.2. Prevailing meteorology:

The climate of Numaligarh and its surrounding areas is sub-tropical with a hot and humid weather prevailing most of the summer and monsoon months. Spring season starts from February and lasts up to end of March (Table 1).

Table 1: Monthly mean (± Standard Deviation) values and ranges of the meteorological parameters in the study area (T=temperature, RF=rainfall, RH=relative humidity, AP=atmospheric pressure, WS=wind speed).

season	T(^{o}c) Mean ± SD Range	RF(cm) Mean	RH(%) Mean ± SD Range	AP(mm) Mean ± SD Range	WS(m/s) Mean ± SD Range
summer	27.08±3.52	110	64.70±3.39	745.06±3.26	6.95±2.38
	38.30-18.10		87-17.2	750.6-737.2	13.4-1.7
Monsoon	25.36± 3.43	137	75.04±2.97	738.13±2.09	6.81±1.85
	36.5-16.20		87.5-26.5	741.8-734.2	10.4-4.1
Autumn	24.75±2.56	90	78.56±2.22	745.13±3.30	3.83±2.29
	32.1-15.10		87.6-49.22	757.6±739.8	9.00-0.1
Winter	19.81±2.47	70	66.35±1.34	750.42±2.70	5.55±2.02
	29.1-8.2		86.4-31	757.2-744.8	10.2-2.0

During this season, brief showers of rain are common along with storms and hailstorms. This is followed by summer up to the month of May. The summer season is followed by monsoon, which starts from June and continues up to September. The precipitation and humidity is highest during this period. The hottest months are

June to August and December & January are the coldest months of the year. Cool breeze blows in the month of October to January making the weather conditions quite pleasant. The autumn season prevails from month of September to October with moderate temperature and rainfall. The winter season prevails from month of November to February, where the daytime mercury reading at this time of the year goes as high as 29.1°C and with minimum 8.2°C at night. During the campaign period, the meteorological parameters, i.e., temperature (°C), rainfall (mm), relative humidity (%), atmospheric pressure (mm), wind speed (m/s), and wind direction (degree) etc. were recorded. The monthly mean (±standard deviation) values and ranges of above meteorological variables are given in Table 1. The prevalent wind direction during winter and spring was north-north-easterly, and south-easterly.

2.3. Sampling:

PM10 samples were collected with PM10 (EcoTech Model AAS 127) was collected in 47 mm diameter glass fiber (EPM2000) filter papers (Whatman). The samplers were placed at sites without any physical obstruction on built platforms of ~ 5 m high above ground level such that vehicle-blown road dusts could be avoided from being collected.

The samplers suck air at a high flow rate of 1.1 – 1.7 m^3 min^{-1} through the appropriate filter paper that retains the particles. The instrument measures the volume of air sampled, while the amount of particulates collected is determined by measuring the change in weight of the filter paper prior to and after sampling. PM concentration is determined from the formula

$$PM\ (\mu g\ m^{-3}) = (W_2-W_1) \times 10^6 / \{(Q_1+Q_2)/2\} \times time$$

Where, W_2 is the weight of the filter paper after sampling (g), W_1 is the weight of the fresh filter paper (g), Q_1 is the initial sampling rate (m^3 min^{-1}), and Q2 is the final sampling rate (m^3 min^{-1}).

Benzo-a-pyrene is designed to collect particulate phase PAHs in ambient air and fugitive emissions and to determine individual PAH compounds. Collected samples through a high volume-sampler (HVS) using glass fibre (EPM2000) filter paper (Whatman) at a flow rate1.2 m^3 min^{-1} over an extended period of 8 hours and subsequent analysis done by using Gas Chromatograph (GC). If sampling period is extended to 24 h without changing the filter, it may enhance sample loss due to volatility or reactions of PAHs on collection media [17, 18].

Punched 30 percent of total sample of the exposed filter paper or measured fraction of it into small strips in a beaker of 250 ml capacity. Added tri-phenyl benzene and add about 100 ml of toluene for extraction and keep beakers in ultrasonic bath for 30 min. Filtered the extracts into evaporative flask of 250 ml with the help of Whatman filter paper. Evaporate the toluene extracts using rotary evaporator with water bath as cool as possible (temperature less than 40^oC). It should be stopped at near dryness (less than 1 ml, visible). Add 2.0 ml of toluene to rinse the wall of evaporation flask and transfer extract into a beaker of 5 ml capacity. Then the extracted solution is run in GC for analysis.

Atomic absorption spectroscopy technique makes use of absorption spectrometry to assess the concentration of Lead and Nickel in the sample. The method is based on active sampling using PM10 high volume sampler and then sample analysis is done by atomic absorption spectrophotometer. Collected samples were placed in microwave (MW) digestion vessels, and appropriate reagents were added sequentially. The vessels were capped, placed in the MW system, and digested. After cooling to room temperature, extracts were diluted using distilled water, and carefully transferred to AAS sample vials for elemental analysis. It was found that the filter materials contributed negligible interference to the analysis.

2.4. Analysis:

Benzo-a-pyrene were analyzed by filtration with rotary evaporator followed by gas chromatography [19,20]. Gas chromatograph was coupled with mass spectrometry (Perkin Elmer Clarus 600C, Singapore). Gas chromatographic (GC) parameters are as follows: Tube oven temp., 300°C and Carrier gas, N_2 at 0.50 ml min^{-1}. Column–Capillary, ultra 2, 25 m x 320µm, 0.17µm; Detector, Flame Ionization Detector (FID) at 320°C; Air & H_2 gas, 400 ml min^{-1} & 40 ml min^{-1}; Oven, Initial temp.: 120°C hold for 2 min to 7.0°C min^{-1} to 300°C hold for 10 min and Retention time for BaP 37.71 min, respectively. Chromatographic grade pure hydrogen and air were used for the FID flame, while pure N_2 was used as a carrier gas. The GC set up was connected to a monitor to store and analyze the output data. Each target compound was identified by its retention time to those obtained

for the calibration standards under specified chromatographic conditions and quantification was accomplished by using multipoint external standard curves [21, 22].

Atomic absorption spectroscopy (AAS) used to analyze acidified samples for heavy metals. In the two years of this study measurements were performed with a Perkin Elmer analyst 200 spectrometer. Acetylene entrained air flame is used. AAS is probably the most frequently used analytical method for the determination of particle-bound heavy metals concentrations in air. In this technique, the analyte is aspirated into an ionising flame that causes a chemical reduction of metal ions to ground state atoms, the light absorption of which is measured.

3. Results and discussion:

3.1 Levels and variation of PM10:

In the present study, the overall variations in PM10 for the two sites for the two year period are given in table 2: S1: 22.68 - 56.47 µg m^{-3} (Year 1), S2: 27.25 - 49.55 µg m^{-3} (Year 1), S1: 34.37 - 57.7 µg m^{-3} (Year 2) and S2: 30.24 – 47.25 µg m^{-3} (Year 2) as shown in Fig. 1.

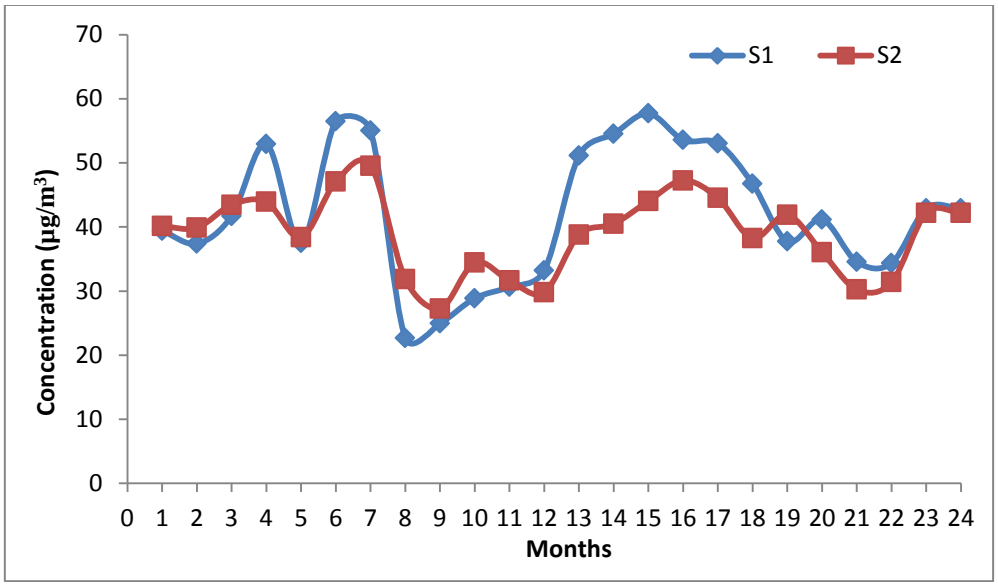

Figure 1: Spatial and monthly distribution trends of PM10 for the two station (Y1=January to December and Y2=January to December).

The seasonal variations are mainly due to the meteorological factors such as relative humidity, temperature and wind speed which favours the dispersion of particulate matter.

Table 2 Spatial (2 sites) and monthly (24 months)variation around Numaligarh refinery along with basic statistics (S1Y1 is S1 site in Year 1 and S1Y2 is S1 site in Year 2, similarly S2Y1 is site S2 in Year 1 and S2Y2 is site S2 in Year 2) [calculated from 24 hourly averages of 9 measurements each month].

Station		PM10 (µgm^{-3})	Lead (µgm^{-3})	Nickel (ngm^{-3})	Benzo a pyrene (ngm^{-3})
S1Y1	Max	56.47	0.20	0.20	0.09
	Min	22.68	0.04	0.04	0.03
	Average	38.39	0.09	0.09	0.06
	Stdev	11.41	0.044	0.05	0.02
S1Y2	Max	57.70	0.18	0.23	0.15
	Min	34.37	0.07	0.06	0.08
	Average	45.85	0.12	0.12	0.11
	Stdev	8.08	0.08	0.06	0.04
S2Y1	Max	49.55	0.18	0.04	0.18
	Min	27.25	0.05	0.02	0.04
	Average	38.11	0.09	0.03	0.11

	Stdev	7.14	0.0330	0.01	0.04
	Max	47.25	0.22	0.15	0.07
S2Y2	Min	30.24	0.07	0.05	0.03
	Average	39.61	0.15	0.08	0.04
	Stdev	5.14	0.04	0.03	0.01

The main anthropogenic sources of the fine particulates, PM10, in Numaligarh can be attributed to vehicular traffic, fossil fuel combustion, and industrial activities that release a large amount of anthropogenic aerosols to the atmosphere. In addition, the boundary layer mixing height is likely to be lower in the study area during the winter due to the low wind speed (2– 10.2 m s^{-1}) and temperatures (2.47–19.81°C) that trap the pollutants near the ground as a result of temperature inversion. Moreover, the winter receives much less rainfall in comparison to the summer. As a result, removal of atmospheric particles by wet scavenging is much reduced in winter than in summer [23, 24]. All of the above explain higher concentrations of PM10 in winter.

The higher relative humidity is known to promote reactions leading to secondary particle formation [25, 26]. It was observed that the relative humidity was much higher in the study area during the summer season compared to that in the winter season and the high relative humidity could have negatively impacted the accumulation of PM in the ambient air. The emissions from the Refinery, the vehicles and other industries in the area, coupled with low wind speed and high relative humidity, have resulted in higher concentrations of PM10 during the months of April and May.

3.2. Levels and variation of benzo-a-pyrene:

An assessment study of Poly aromatic Hydrocarbon concentration in study area was investigated. Monitored concentrations and statistical summary data from the two monitoring sites for benzo-a-pyrene are listed in Table 2. At site S1, the monthly average annual concentration ranged from 0.08 – 0.16 ng m^{-3} with yearly average of 0.11 ng m^{-3}; the value of 0.16 ng m^{-3} is the highest value reported for winter season, which is located in near refinery area. Benzo-a-pyrene is now a day found in ambient air. They are formed due to incomplete combustion of organic matter, and important sources are transport, electricity and heating generation [27, 28]. Such values may indicate that significant fractions of Benzo-a-pyrene at the time of sampling originated from non-traffic related sources. The concentration sources were highly dependent on the humidity of air. The value of 0.08 ng m^{-3} is the lowest value reported for summer season. At lower temperatures, main sources of BaP are most likely originating from power plants and residential heating, most of which still use coal as a fuel. In Y2, the monitoring site with the higher annual average of BaP was near refinery point i.e. S1. Monitored levels at this site have slightly decreased over the past year (Fig. 2);

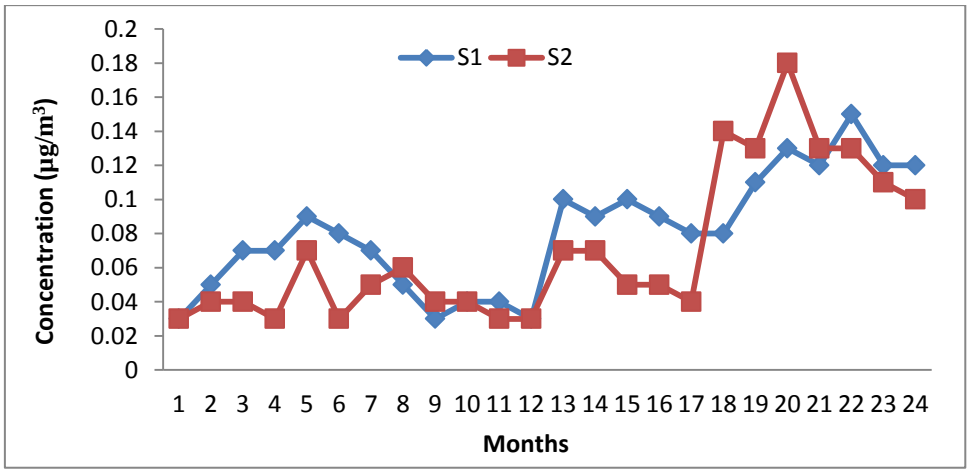

Figure 2: Spatial and monthly distribution trends of Benzo-a-pyrene for the two station (Y1=January to December and Y2=January to December).

the annual average in Y1 was of 0.11 ng m^{-3}, which has decreased to an annual average of 0.05 ng m^{-3} in Y2 with standard deviation 0.02 ng m^{-3}. Annual averages have also decreased at the S2 monitoring site. In Y1, the highest monthly average was in month of August 0.19 ng m^{-3} and lowest April 0.03 ng m^{-3} with yearly average

concentration of 0.10 ng m^{-3}, which is higher, compared to successive years (0.04 ng m^{-3} in Y2). It is important to note that all of these annual averages are still well below the permissible limit, and are not expected to cause adverse health effects. The BaP content in general was richer in the S1 region than in the S2 site where a national highway passed by. The concentrations are below 1 ng m^{-3} set by CPCB. Poly aromatic hydrocarbon elevated concentration is due to traffic occurs mainly at short distances from the road. Increased PAH concentrations may occur in connection with long-range transport, but there are also events with increased concentrations caused by local sources such as wood burning [29, 30] and road traffic exhaust provides an increased local contribution of PAH, and emission from road traffic is the major source of PAH now a days. Emissions of BaP have minimal value in the area and can consider the source with the increase in emissions from household combustion of biomass. At the same time, climate changing policies are promoting the use of biomass burning for domestic heating. The studied samples are categorized to have low degree of contamination which indicates very low anthropogenic pollution at these sites.

3.3. Levels and variation of lead and nickel:

The concentration from the two sites significantly varied from season to season. The annual average concentration of Lead at S1 site is 0.09 µg m^{-3} for Y1 and 0.12 µg m^{-3} for Y2. For S2 site the annual average concentration is 0.09 µg m^{-3} and 0.15 µg m^{-3} respectively for both the year. Spatial and monthly distribution trends of Lead for the two sites are shown in Fig. 3.

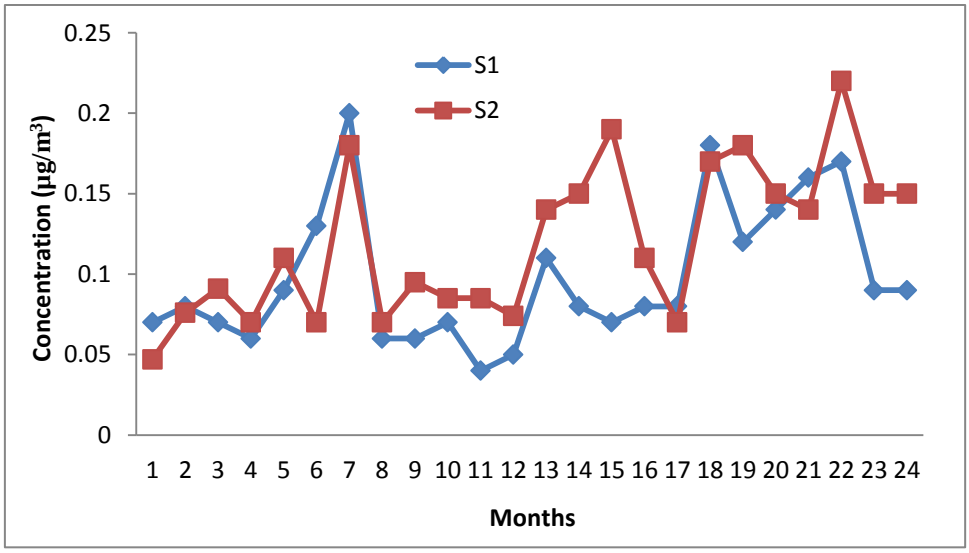

Figure 3: Spatial and monthly distribution trends of Lead for the two station (Y1=January to December and Y2=January to December).

Many industry plants that resulted in pollution were closed to refinery area are brick industries, stone crusher and tea factories.

Lead concentrations were the highest during the first year in month of June (0.18 µg m^{-3}) at S1 with standard deviation of 0.05 µg m^{-3} (Fig 3).These heavy elements have probably the same emission source which is road traffic; the ambient concentration of lead in air shows regional and seasonal differences that depend on the dominant sources and their spatial distribution and on weather and dispersion patterns. We can see the elevated concentration during summer season as during Year 2 highest value is 0.21 µg m^{-3} for the month of July at S1 site. For the site S2 highest value can be observed during the month of October 0.23 µg m^{-3} and July 0.18 µg m^{-3} (Y1 and Y2 respectively).

Lead is present in outdoor air in the form of fine particles with a size distribution characterized by a mean aerodynamic diameter of less than 1 µm. Although lead is removed from the air via wet and dry deposition, mostly near the sources, tiny aerosol particles are involved in the long-range transport of this pollutant. Along with biomass burning, Pb in the samples represented the contributions of other anthropogenic sources such as coal burning and industrial emissions [31]. Coal combustion is the predominant source of toxic metals. Southeast Asia has been cited to contribute significantly to biomass burning pollution worldwide. In the study,

we have identified high Pb episodes during the north easterly monsoon primarily originating from long range transport of the Assam pollution outflow, and the sources of aerosol Pb primarily localized around the refinery area.

The main sources of lead production are industrial production (lead is present as a secondary constituent in many minerals and sediments) and coal combustion (domestic combustion and heating and electricity plants). Motor vehicles (alkyl-lead additives in petrol) are an important mobile source of lead released into the air in countries where leaded petrol is used. As this source is near the population and widely distributed, road traffic is a major source of exposure. The Pb concentration is lower in S2 site compared to S1 site throughout the monitoring period. This may be due to absence of such industrial plants in that study area; long-range transport phenomena can explain the presence of such elements.

Similarly for Nickel the annual average for S1: 0.08 ngm^{-3} (Y1), 0.12 ng m^{-3} (Y2) and S2: 0.03 ng m^{-3} (Y1), 0.08 ng m^{-3} (Y2) respectively. Spatial and monthly distribution trends of Nickel for the two sites are shown in Fig. 4.

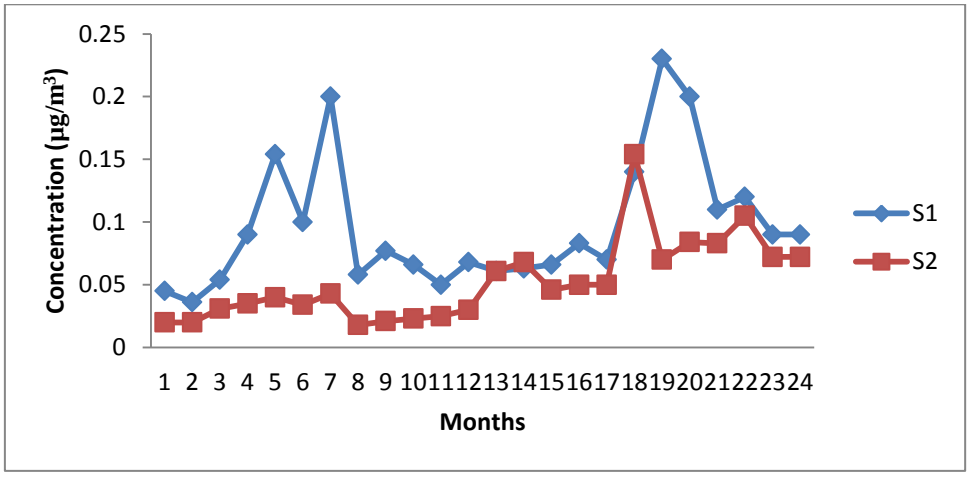

Figure 4: Spatial and monthly distribution trends of Nickel for the two station (Y1=January to December and Y2=January to December).

The highest concentration at site S1 for both the year can be seen during the month of July with value of 0.20 ng m^{-3} and 0.23 ng m^{-3}. Elevated Ni levels were attributed to petroleum refinery as well as effluents from a variety of factories and industrial facilities. A winter maximum of Ni was attributed to the enhancement of combustion activities [23]. A higher concentration of Ni was observed at the industrial site than the residential site. Industrial metallurgical processes and combustion of diesel oil are the major sources of Ni [32]. All the concentrations are much below the permissible limits i.e. 20 ng m^{-3} set by NAAQM standards. Nickel concentration for S2 site can be observer highest in the month of July (0.04 ng m^{-3}) for Y1 and June (0.15 ng m^{-3}) for Y2 as shown in Fig. 4. The variations in the concentration at the S2 site could be explained on the basis of differences in the environmental situation, influence of regional meteorology over local events and sources, etc. This short of concentration during the study period can be attributed to vehicular exhaust because of its use as an additive in fuel. Ni concentrations in PM10 between spring and summer sampling periods, were spring season is lower from summer season. This factor is associated with coal-oil combustion (Zn, Mn, Ni) and traffic emission sources (Zn, Pb, Cu, Cd, and Ni) [33].

The Ecological risk factor of heavy metal was considered as the sum of the pollutant caused by heavy metal. Ecological risk factor characterized sensitivity of local ecosystem to the toxic metals and represent ecological risk resulted from the overall contamination. There is very low degree of contamination, this indicates that the Ecological risk factor in all the studied sites indicate low ecological risk [34].

4. Air quality modeling and air pollution impact:

The ground level concentration (GLC) of pollutants due to emissions from stationary elevated sources is computed using dispersion models, which are mathematical relations between the source strength and

concentration and involves parameters related transport and diffusion. The empirical Gaussian model is the widely used model in practice which assumes that the parameters governing the transport and diffusion do not change in space and time. For the present study, BREEZE AERMOD, a new generation air quality modeling system is used. AERMOD is an EPA model approved by USEPA for predicting the dispersion of airborne pollutants from a source, in this case refinery, brick kiln and tea factories. We applied AERMOD to compare the measured PM concentrations to those predicted as a function of our calculated emissions. These models provide quite conservative results to have sufficient safety cushion for decision making.

It is known that impact of air pollution is dependent on meteorological conditions. As meteorological conditions change significantly from season to season we have assessed air pollution for different seasons and also for the whole year. For air pollution impact, we have considered two major seasons - winter and summer - and annual average. As our pollution standards are given as 24 hour averages and annual averages, both 24 hour averages and seasonal averages have been considered.

The AERMOD predictions exhibit a PM spatial distribution consistent with our field measurements and validate our hypothesis that emission from refinery, brick kiln and tea factories are the source of PM in the nearby surrounding areas. The results of AERMOD program run for refinery sources are given below. Maximum Predicted Winter Season 24 hour Average increase in GLC for PM is 1.58 µg m^{-3} (Fig. 5).

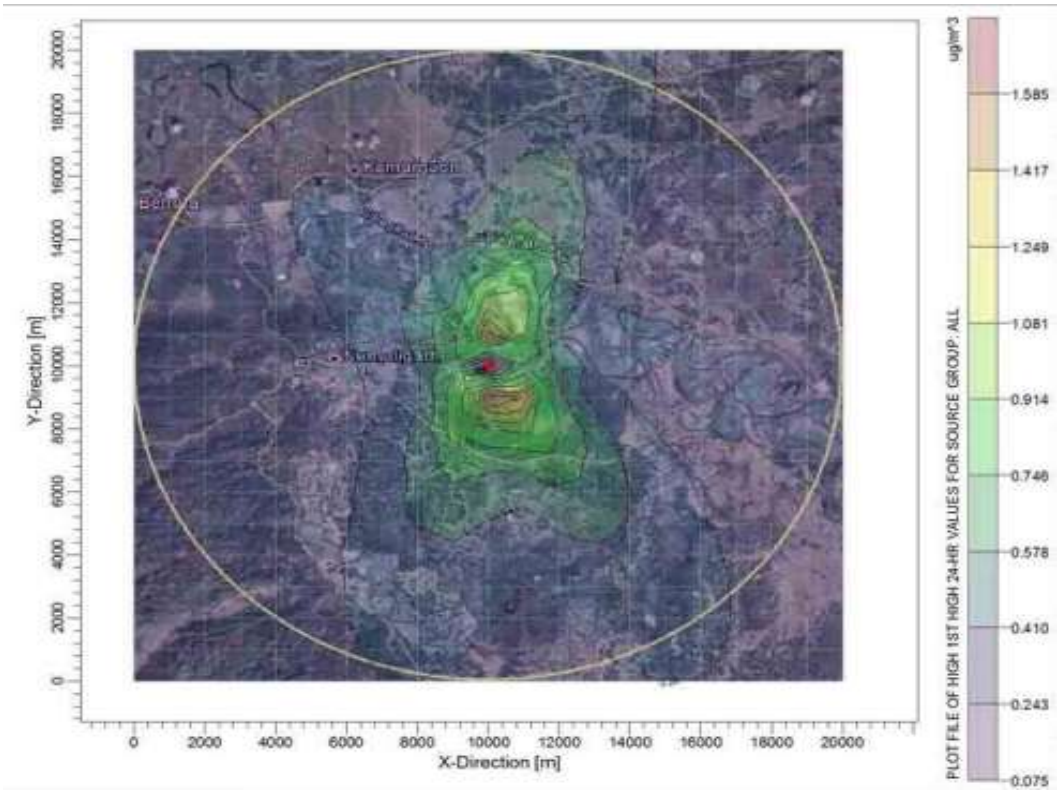

Figure 5: Shows the 24 hour average maximum increase isopleths in winter for PM on the satellite map of the area.

It can be seen that the maximum increases are all very minimal. If we consider the seasonal average then the increases are nearly negligible. The contours show that in most of the area increase in GLC of pollutants are negligible. Only in a very small pocket there is marginal increase.

Maximum Predicted Winter Season Average increase in GLC is 0.19 µg m^{-3} (Fig. 6). The contours show that in most of the area increase in GLC of pollutants are negligible. Only in a very small pocket there is marginal increase. Maximum Predicted Summer Season 24 hour Average increase in GLC is 2.05 µg m^{-3}(Fig. 7). The maximum Predicted Summer Season Average increases in GLC 0.55 µg m^{-3} (Fig. 8) and 24 hour annually average increase in GLC is 1.97 µg m^{-3} (Fig. 9). Maximum Predicted Annual Average increases in GLC 0.45 µg m^{-3} (Fig. 10).

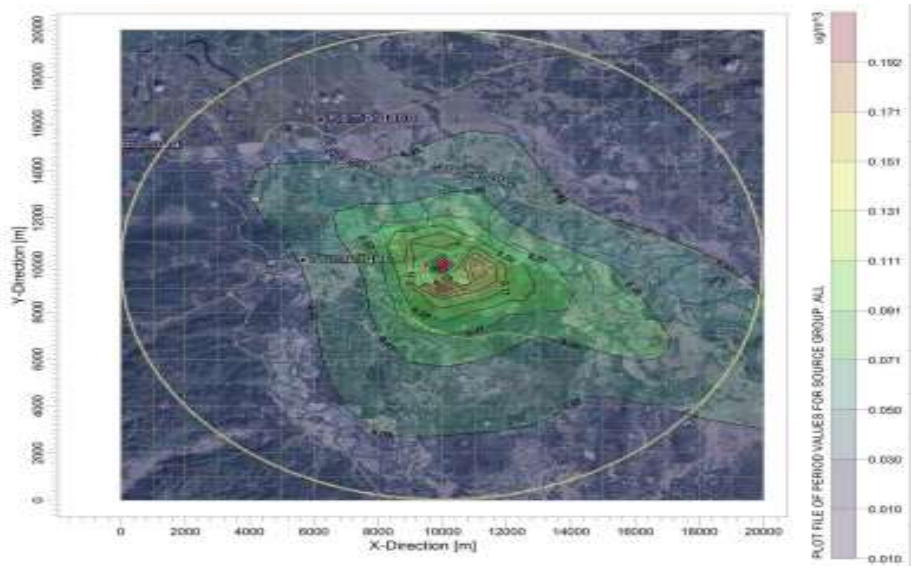

Figure 6: Shows the winter season average increase isopleths in winter for PM on the satellite map of the area.

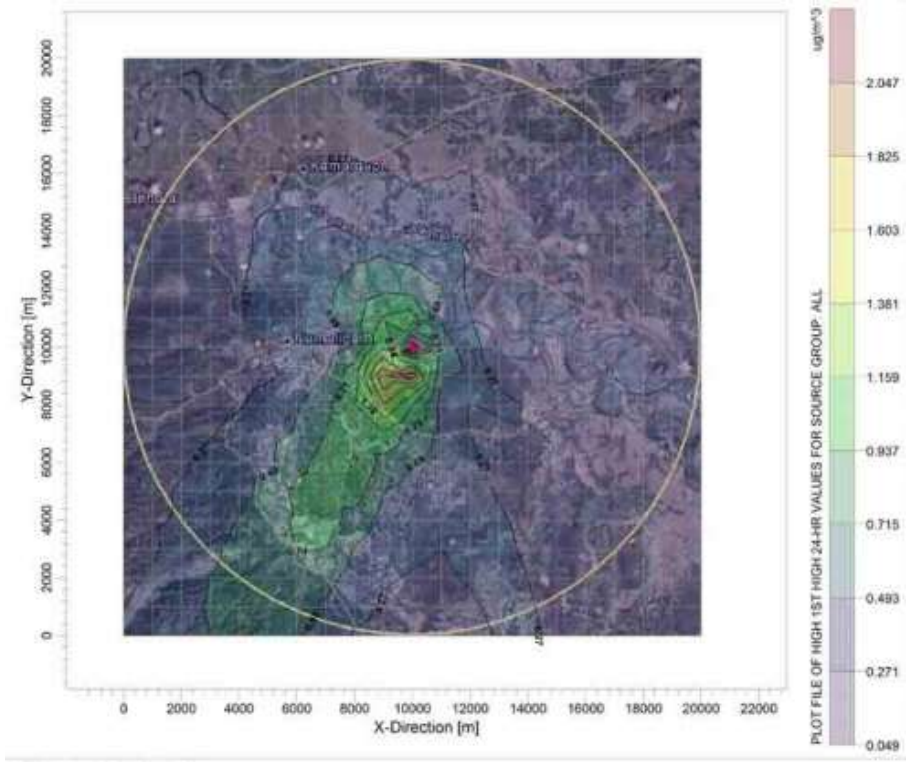

Figure 7: Shows the 24 hour average maximum increase isopleths in summer for PM on the satellite map of the area.

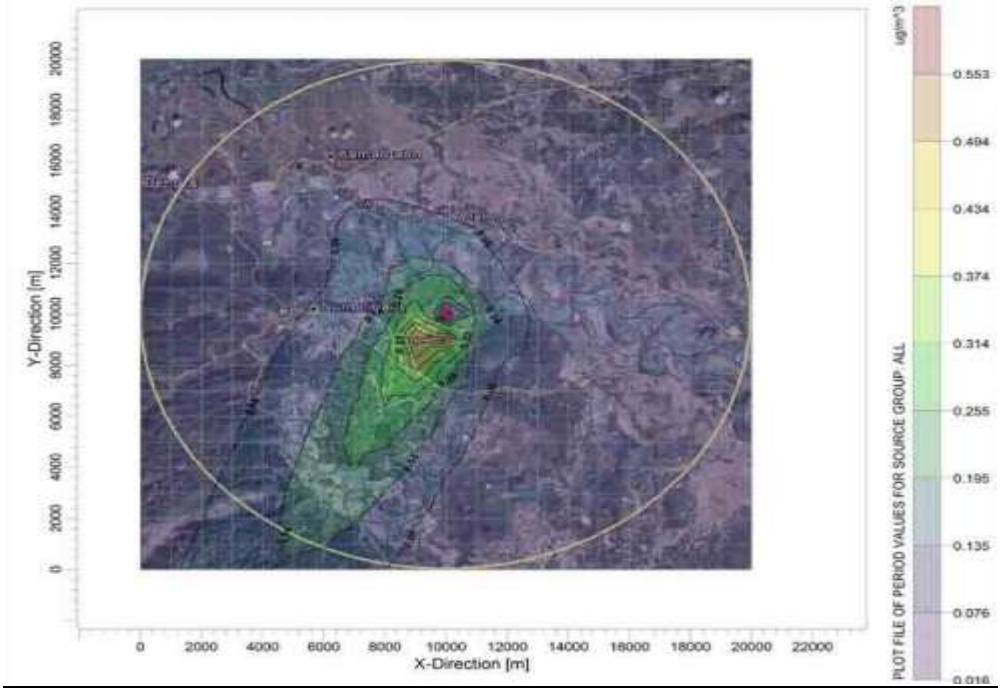

Figure 8: Shows the summer season average increase isopleths for PM on the satellite map of the area.

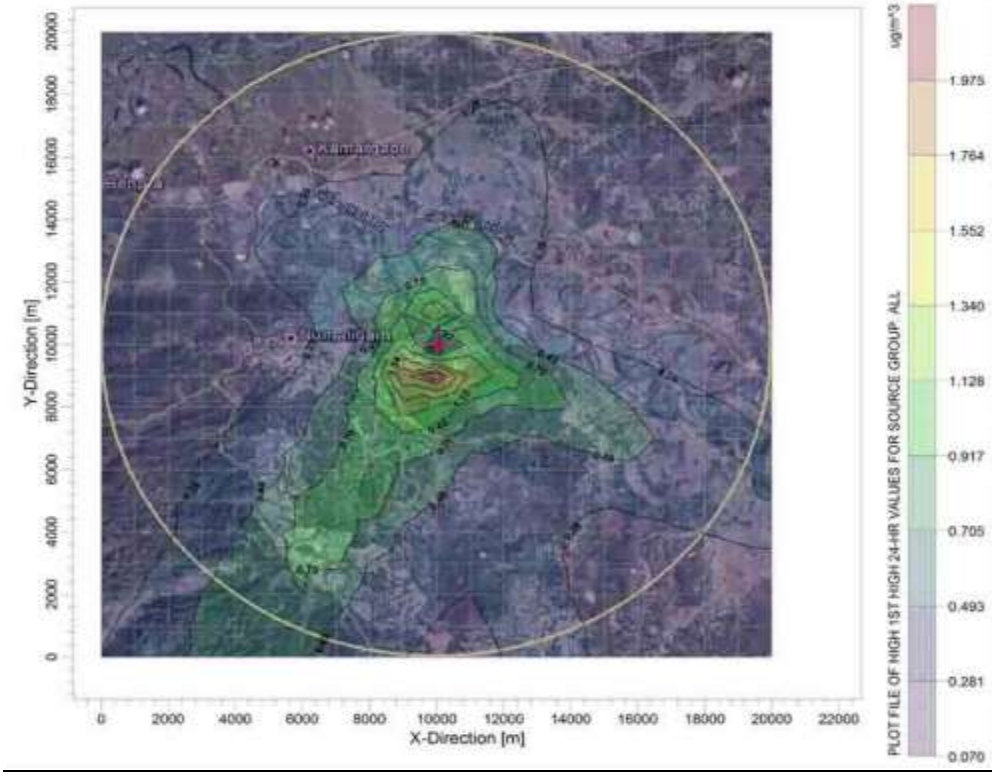

Figure 9: Shows the Annual 24 hour average maximum increase isopleths for PM on the satellite map of the area.

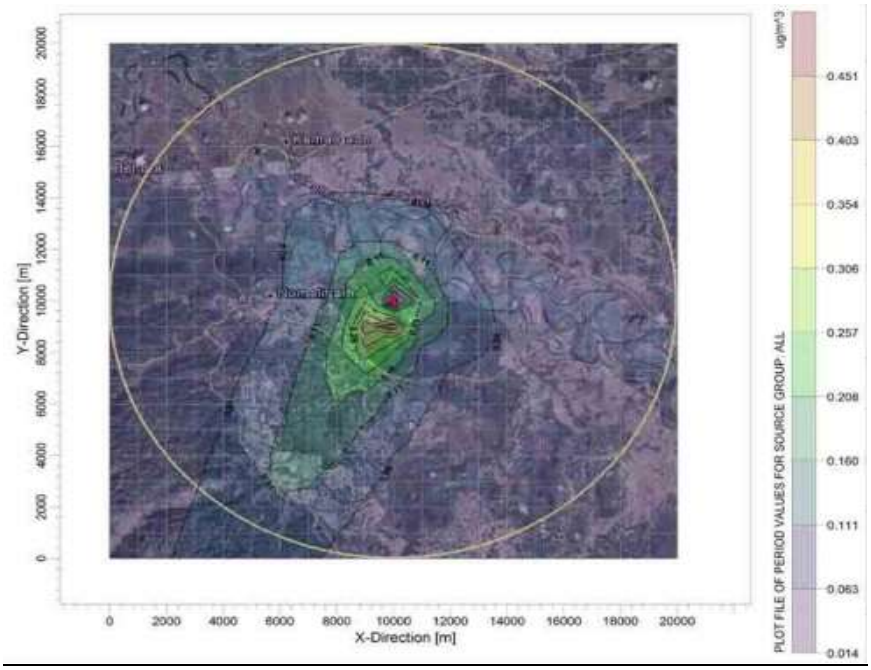

Figure 10: Shows the Annual average increase isopleths in winter for PM on the satellite map of the area.

4.1. Impact from area source:

It has been mentioned that there are a number of tea estates and brick kilns functioning in the impact zone. As their exact locations could not be identified for all, we have decided to distribute these sources evenly in the study region. A 10km x 10 km impact zone is selected and the area is equally divided into 2km x 2km grids, totally 25 squares. One tea estate and one brick kiln are considered to be located at the centre of each square.

BREEZE AERMOD is again run for the area source scenario for the winter season as described above. Area Sources - Max. Predicted Winter Season 24 hour Average Increase in GLC 6.71 μg m^{-3} (Fig. 11).

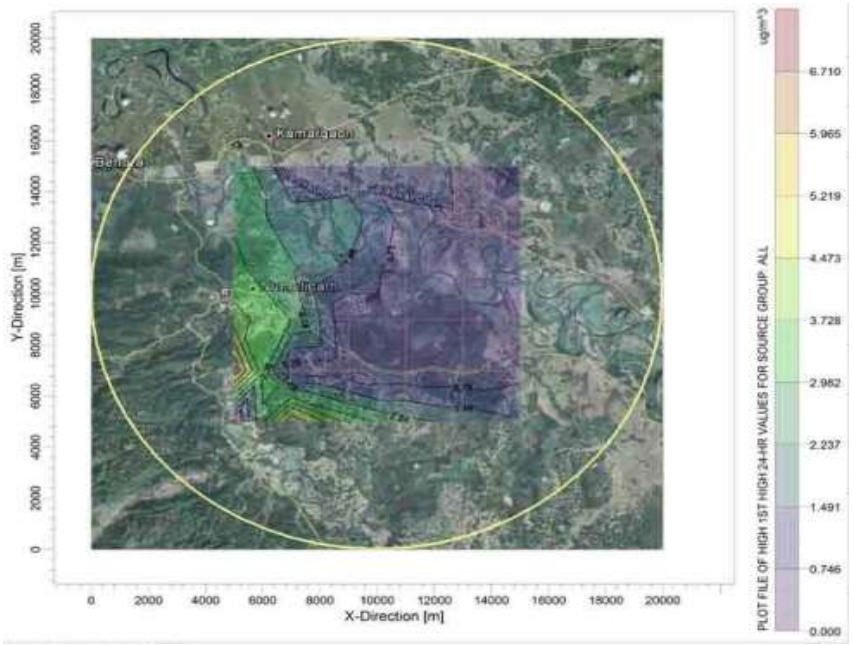

Figure 11: Shows the 24 hour average maximum increase isopleths in winter for PM on the satellite map of the area

The contours show that in most of the area increase in GLC of pollutants are negligible. Only in a very small

pocket there is marginal increase.

Area Sources - Maximum Predicted Winter Season Average increase in GLC 0.45 µg m^{-3} (Fig. 12).

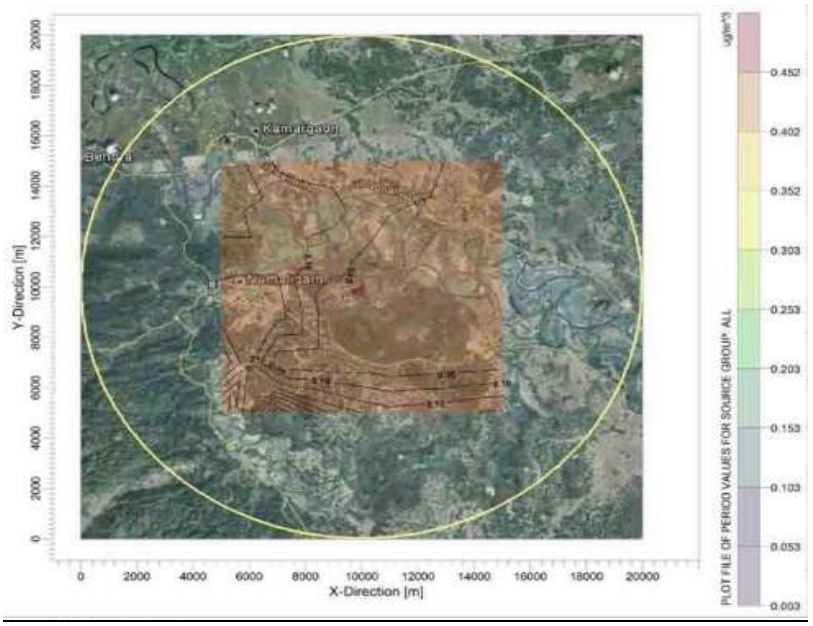

Figure 12: Show the winter season average increase isopleths for PM on the satellite map of the area.

The GLC contours are plotted in the area 10 km x 10 km. It can be seen that in most of the region increase in GLC is negligible, except marginal increase in a few pockets.

Area Sources - Maximum Predicted Summer Season 24 hour Average as well as Summer Season Average increase in GLC are 5.68 µg m^{-3} (Fig. 13) and 0.13 µg m^{-3} (Fig. 14) respectively. Area Sources - Max. Predicted Annual 24 hour Average along with Annual Average increase in GLC are 6.21 µg m^{-3} (Fig. 15) and 0.28 µg m^{-3} (Fig. 16).

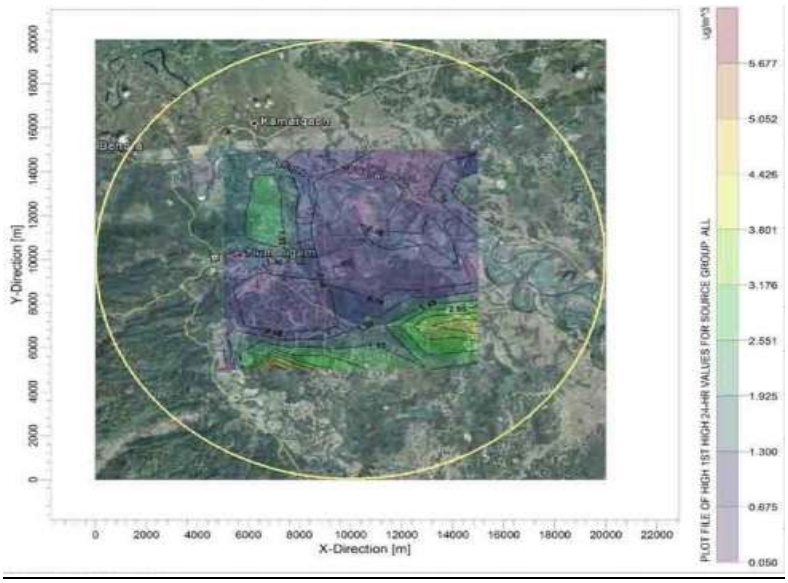

Figure 13: Shows the 24 hour average maximum increase isopleths in summer for PM on the satellite map of the area.

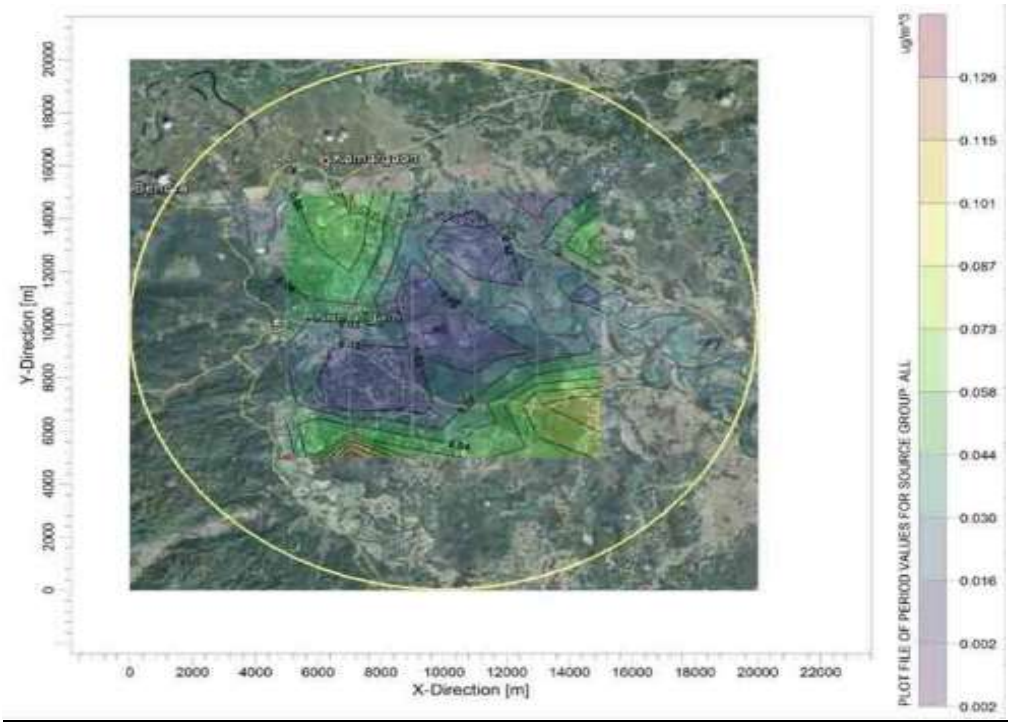

Figure 14: Shows the summer season average increase isopleths for PM on the satellite.

Figure 15: Show the Annual 24 hour average maximum increase isopleths for PM on the satellite map of the area.

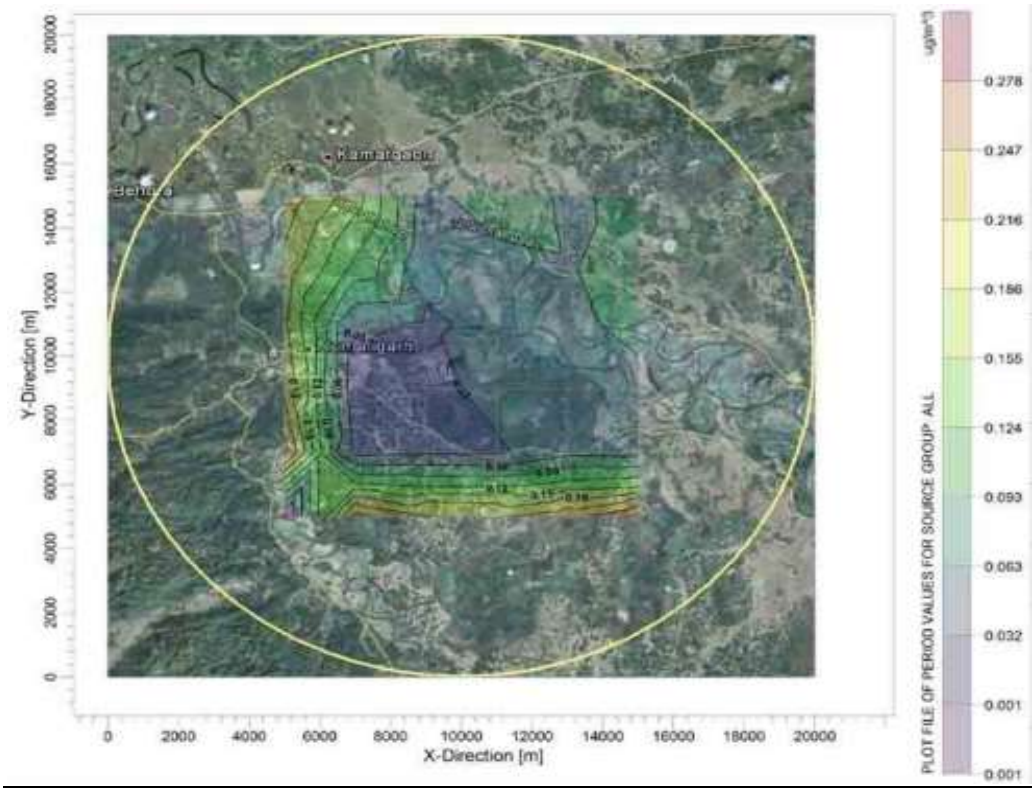

Figure 16: Show the Annual average increase isopleths for PM on the satellite map of the area

4.2. Implication:

The results of this study support our working hypothesis: PM emissions from refinery explain nearby air concentrations. Specifically, we cite three independent findings. First, we note the large spatial variation in measured airborne particulate matters, with much concentration close to the shoreline. Second, we found that the profiles of PM congeners in the air samples are remarkably similar. The similarities are strongest for air samples collected close to the shoreline. Third, we found that our predicted and measured air concentrations exhibit similar ranges of values and similar spatial distributions. To the best of our knowledge, this is the first study to show that a PM contaminated ambient air is responsible for the nearby measured particulate matters.

It is likely that PMs have been emitted from different sources for many years. Our findings indicate that PM is the source for ongoing occurrence of airborne Benzo-a-pyrene and heavy metals in the Numaligarh area and the cause of the minute concentrations in the neighbourhood surroundings.

5. Health risk assessment:

5.1. Exposure calculation:

The benzene and benzo-a-pyrene concentrations were converted from μgm^{-3} to µg/kg/day in terms of Lifetime Average Daily Dose (LADD) using values summarized in Table 3.

Table 3: Summary of default exposure factors.

Parameters	Unit	Default values
Lifetime (LT)	Years	70
Bodyweight (BW)	Kg	70
Exposure length (EL)	Day/day	0.33(8hr/day)
Exposure duration (ED)	Years	25(commercial/industrial)
Inhalation rate (IR)	M3/day	20
Inhalation reference dose(Rfd)	µg/kg/day	0.0085
Slope factor	$(\mu g/kg/day)^{-1}$	0.0273

The LADD were used in calculating the Hazard Quotient (HQ) and Cancer Risk (CR). The values of USEPA Inhalation Reference Dose (RfD) and Slope Factor (SF) for estimating the HQ and CR were summarized in Table 3 [35, 36]. The Lifetime Average Daily Doses (LADD) (µg/kg/day) for exposure to Benzo-a-pyrene concentrations was calculated for both Station using the default values in Table 3 and 4.

$$LADD = [Cexp \times IR \times EL \times ED] / [BW \times LT]$$

Where Cexp is exposure concentration (µg m^{-3}); IR, Inhalation Rate (m^3 day^{-1}); EL, Exposure Length (day day^{-1}); ED, the Exposure Duration (days); BW, Body Weight (kg); LT, Lifetime (days).

Table 4: Health risk characterization for exposure to Benzo a pyrene (S1Y1 is S1 site in Year 1 and S1Y2 is S1 site in Year 2, similarly S2Y1 is site S2 in Year 1 and S2Y2 is site S2 in Year 2).

Station	Cexp (µgm^{-3})	LADD	HQ	CR
S1Y1	$0.06*10^{-3}$	$0.55*10^{-8}$	$65.29*10^{-8}$	$0.02*10^{-8}$
S1Y2	$0.11*10^{-3}$	$1.02*10^{-8}$	$119.71*10^{-8}$	$0.03*10^{-8}$
S2Y1	$0.11*10^{-3}$	$1.02*10^{-8}$	$119.71*10^{-8}$	$0.03*10^{-8}$
S2Y2	$0.042*10^{-3}$	$0.39*10^{-8}$	$45.71*10^{-8}$	$0.01*10^{-8}$

5.2. Hazard quotient (HQ):

The HQ method of risk characterization was used to estimate the adverse health effects for exposure to Benzo-a-pyrene. The USEPA Reference Dose (RfD) derived for Benzo-a-pyrene was used to estimate the HQ for all sampling site. HQ was estimated by using following equation

$$HQ = LADD / RfD$$

Where HQ is the Hazard Quotient; LADD, lifetime average daily dose (µg/kg/day); RfD, USEPA reference dose (µg/kg/day) (Table 3 and 4).

5.3. Cancer risk (CR).

Cancer risk is expressed as excess risk of developing cancer over a lifetime of exposure (70 years). The USEPA inhalation slope factor derived for benzene was used to quantitatively estimate the excess cancer risk in terms of lifetime exposure (LADD) by using Equation:

$$\text{Cancer Risk} = LADD\ (\mu g/kg/day) \times SF\ (\mu g/kg/day)^{-1}$$

Where SF is slope factor for Benzo-a-pyrene (Table 3 and 4).

The excess cancer risk in terms of lifetime exposure to BaP is very low in the range of 0.01×10^{-8} to 0.03×10^{-8} which is far less than the value 0.25×10^{-8}. USEPA (United States environmental protection agency) uses mathematical models, based on human and animal studies, to estimate the probability of a person developing cancer from breathing air containing a specified concentration of a chemical. USEPA calculated a range i.e. 0.22 to 0.78 ng m^{-3} as the increase in the lifetime risk of an individual who is continuously exposed to above 1 ng m^{-3} of BaP in the air over their lifetime [37]. EPA estimates that, if an individual were to continuously breathe the air containing BaP at an average of 0.13 to 0.45 µg m^{-3} over his or her entire lifetime, that person would theoretically have no more than a one in-a-million increased chance of developing cancer as a direct result of continuously breathing air containing this chemical.

4. Conclusions:

The aim of our study was to modelling and applies a methodology to determine and calculate the LADD, HQ and CR values associated with the different pollutants sought and found in the study area. The ecological risks of the BaP and heavy metals were assessed based on their adverse ambient effects by using the reference recommended by the National ambient air quality monitoring standard. The results indicated that the ecological risks of BaP, Pb and Ni in ambient air from Numaligarh were very low. Being semi-volatile in nature they are partitioned between gas and particulate phases which controls their lifetime, deposition, chemical transformation and transport potential both in the atmosphere and the human body. The study demonstrates that the concentration of PAHs is influenced by temperature while their partitioning is governed by adsorption processes. The contamination of studied sites has not been to the level where immediate intervention would be needed ameliorate pollution. All these toxic substances were impotent in the study area.

References:

[1] Peng S, Zhou R, Qin x, Shi H, Ding D (2013) Application of macrobenthos functional groups to estimate the ecosystem health in a semi-enclosed bay. Mar Pollut Bull 74:302–310.
[2] Robertson A (1998) Arctic Monitoring and Assessment Programme (AMAP), Oslo, Norway. 661-716
[3] Anejionu OCD, Ahiarammunnah PAN, Nri-ezedi CJ (2015) Resources policy. 45:65-77.
[4] Maziejuk M, Szczurek A, Maciejewska M, Pietrucha T, Szyposzyńska M, (2016) Determination of benzene, toluene and xylene concentration in humid air using differential ion mobility spectrometry and partial least squares regression. Talanta 152:137-146.
[5] Brook RD, Rajagopalan S, Pope 3rd CA, Brook JR, Bhatnagar A, Diez-Roux AV, Holguin F, Hong Y, Luepker RV, Mittleman MA, Peters A, Siscovick D, Smith Jr SC, Whitsel L, Kaufman JD (2010) Particulate matter air pollution and cardiovascular disease: an update to the scientific statement from the American Heart Association, Circulation 121:2331–2378.
[6] Donaldson K, Seaton A (2012) A short history of the toxicology of inhaled particles. Part Fibre Toxicol 9:13.
[7] Kim KH, Kabir E, Kabir S (2015) A review on the human health impact of airborne particulate matter. Environ Int 74:136–143.
[8] Galadima A, Garba ZN (2012) Heavy metal pollution in Nigeria: Causes and consequences. Elixir J Poll 45:7917–7922.
[9] Duong TT, Lee BK (2011) Determining contamination level of heavy metals in road dust from busy traffic areas with different characteristics. J Environ Manage 92:554–562.
[10] Modrzewska B, Wyszkowski M (2014) Trace metals content in soils along the state road 51 (Northeastern Poland). Environ Monit Assess 186:2589–2597.
[11] Rijkenberg MJ, Depree CV (2010) Heavy metal stabilization in contaminated road-derived sediments. Sci Total Environ 408:1212–1220.
[12] Wei B, Jiang F, Li X, Mu S (2009) Spatial distribution and contamination assessment of heavy metals in urban road dusts from Urumqi, NW China.Microchem J 93:147–152.
[13] San Miguel G, Fowler GD, Sollars CJ (2002) The leaching of inorganic species from activated carbons produced from waste tyre rubber. Water Res 36:1939–1946.
[14] Lindgren S (1996) Asphalt wear and pollution transport. Sci Total Environ 189: 281–286.
[15] Liu Q, Liu Y, Zhang M (2012) Mercury and cadmium contamination in traffic soil of Beijing, China. B. Environ Contam Tox 88:154–157.
[16] Kummer U, Pacyna J, Pacyna E, Friedrich R (2009) Assessment of heavy metal releases from the use phase of road transport in Europe. Atmos Environ 43:640–647.
[17] CPCB Guidelines for ambient air quality monitoring. Report under Central Pollution Control Board, Ministry of Environment, Forest and climate change, Government of India, 2009.
[18] CPCB, 2011. Air quality monitoring, emission inventory and source apportionment study for Indian cities.
[19] Brown R H (1998) Environmental Carcinogenic Methods of Analysis & Exposure Measurement, Benzene and Alkylated Benzene, vol. 10, edited by L O Fishbein & J K Neill (Oxford University Press, London, UK) 235-242.
[20] Montells R, Aceves M, Grimalt O (2000) Sampling and analysis of volatile organic compounds emitted from leaded and unleaded gasoline powered motor vehicle. Environ Monit Assess 62:1-14.
[21] Caldwell ME, Suflita JM (2000) Detection of phenol and benzoate as intermediates of anaerobic benzene biodegradation under different terminal electron accepting condition. Environ Sci Technol 34:1216-1220.
[22] US Environmental Protection Agency (1999) Compendium Method TO-17, Determination of volatile organic compounds (VOCs) in ambient air using active sampling onto sorbent tubes, EPA 625/R-96/010b (Office of Research and Development, Cincinnati, OH, 45268): 1-50.
[23] Karar K, Gupta AK (2006) Seasonal variations and chemical characterization of ambient PM10 at residential and industrial sites of an urban region of Kolkata (Calcutta), India. Atmospheric Research 81:36-53.
[24] Deshmukh DK, Deb MK, Tsai YI, Mkoma SL (2010) Atmospheric ionic species in PM2.5 and PM10 aerosols in the ambient air of eastern central India. Journal of Atmospheric Chemistry 66:81-100.
[25] Cheng Y, He KB, Du ZY, Zheng M, Duan FK, Ma YL (2015) Humidity Plays an Important Role in the PM2.5 Pollution in Beijing. Environmental Pollution 197:68-75.
[26] Zhou Y, Cheng S, Chen D, Lang J, Wang G, Xu T, Wang X, Yao S (2015) Temporal and Spatial Characteristics of Ambient Air Quality in Beijing, China. Aerosol and Air Quality Research 15:1868-1880.
[27] Carlsen L, Kenessov B, Baimatova N (2013) Assessment of the air quality of Almaty. Focussing on the traffic component. Int J Biol Chem 49:49–69.

[28] Liu K, Zhang C, Cheng Y, Liu C, Zhang H, Zhang G (2015) Serious BTEX pollution in rural area of the North China Plain during winter season. J Environ Sci 30:186–190.
[29] Ovri JEO, Iroh M (2013) Corrosion effect of gas flaring on galvanized roofing sheet in Imo State, Nigeria. Int J Eng Sci 2(1): 339–345.
[30] Oros DR, Ross JRM (2004) Polycyclic aromatic hydrocarbons in San Francisco Estuary sediments. Marine Chemistry 86:169-184.
[31] Christian TJ, Yokelson RJ, Cardenas B, Molina LT, Engling G (2010) Trace gas and particle emissions from domestic and industrial biofuel use and garbage burning in central Mexico. Atmos Chem Phys 10:565–584.
[32] Nikolaos S, Thomaidis B, Evangelos B, Bakeas A, Panayotis A, Siskos (2003) Characterization of lead, cadmium, arsenic and nickel in PM2:5 particles in the Athens atmosphere, Greece. Chemosphere 52:959–966.
[33] Constantini S, Demetra V (2005) Size distribution of airborne particulate matter and associated heavy metals in the roadside environment. Chemosphere 59: 1197–1206.
[34] Suleiman MB, Salawu K, Barambu AU (2019) Assessment of concentration and ecological risk of heavy metals at resident and remedial soils of uncontrolled mining sites at Dareta village, Zamfara, Nigeria. J Appl Sci Environ Manage 23(1):187 – 193.
[35] Adjagbo K, Loranger S, Moore S, Tardif R, Sauvé S (2010) Hum Ecol Risk assess Int J 16:301–316.
[36] United State Environmental Protection Agency. Risk Assessment Guidance for Superfund: Human Health Evaluation Manual Supplemental Guidance "Standard Default Exposure Factors"; OSWER Directive: Washington, DC, USA (1991) Volume 1:pp. 1–1.
[37] U.S. Environmental Protection Agency. Integrated Risk Information System (IRIS) on Benzene. National Center for Environmental Assessment, Office of Research and Development, Washington, DC. 2009.